https://doi.org/10.46813/2025-158-003

EXPERIMENTAL STUDY OF PLASMA OPENING SWITCH IN ELECTRON ACCELERATOR WITH INDUCTIVE ENERGY STORAGE

D.V. Vinnikov[1,2], O.M. Ozerov[1], V.V. Katrechko[1], V.I. Tkachov[1], S.V. Marchenko[1], V.B. Yuferov[1], O.V. Manuilenko[1], I.N. Onishchenko[1]
[1]National Science Center "Kharkiv Institute of Physics and Technology", Kharkiv, Ukraine;
[2]O.Ya. Usikov Institute for Radiophysics and Electronics National Academy of Sciences, Kharkiv, Ukraine
E-mail: vinniden@gmail.com

An experimental study of the plasma opening switch (POS), its dynamics and current characteristics was carried out using a small-size electron accelerator of direct action with inductive energy storage (IES). The methods for determining the induced voltage based on experimental current oscillograms have been used. Characteristic current oscillograms have been obtained. Values of the charging voltage and current for the main circuit have been established to provide a maximum induced voltage and the best multiplication factors. The effect of the charging voltage of the circuit of plasma gun (PG) and the number of PGs on the voltage multiplication has been established. Optimal delay times between the operation of the PGs and the pulse current generator (PCG) of the main circuit have been determined. The effect of inductance on the multiplication factor has been determined. Current beams with values exceeding those of the limiting vacuum current have been obtained for the selected diode geometry.

PACS: 52.75.−d, 94.20.wc, 52.80 Vp, 52.70Kz, 29.30Ep

INTRODUCTION

The direct-action electron accelerators with the IES and POS are used in the fields that require small overall dimensions and appropriate weight characteristics that ensure the maneuverability and the possibility of placement on moving platforms. A wide range of applications justify the demand for accelerators of this type and the global interest of scientists in such accelerators [1, 2].

The DIN-2K accelerator is a laboratory prototype of the systems of this type. It is currently used for the study of electron beams, virtual cathodes, the combined effects of ionic and electron radiation on structural materials and other appropriate phenomena [3 - 14].

This paper delves into the dynamics of the current charging the inductive line. The dynamics of so-called total current that exists during the conduction phase in the coaxial line when the POS has not triggered yet, the transfer of energy from the capacitive storage device, in our case from the PCG to the inductive storage device, when the POS remains open, and the change of the current and voltage induced during the POS triggering have been studied. The voltage induced in the IES with POS due to plasma current interruption is the key factor providing the possibility for explosive emission from the cathode and, consequently, the electron beam and the virtual cathode that is the source of the electromagnetic radiation. Thus, specifying the factors that effect and enable the control of the value of induced voltage is an important task that ensures the successful implementation of many technological processes under consideration.

The objectives of this research are to establish the optimal ranges for parameters of the primary circuit of the PCG and the circuit of PGs used by the high-current linear accelerator DIN-2K that guarantees the maximum values of the induced voltage and origination of the electron beam.

1. DESCRIPTION OF THE SYSTEM OPERATION

A general view and schematic diagram of a small-size direct-action electron accelerator DIN-2K equipped with IES and POS is shown on Fig. 1 (right). The electrical circuit diagram of the accelerator is shown in Fig. 2. When the plasma guns are triggered, the plasma is created, and after the set delay time, the PCG of the main circuit is actuated and the main circuit current I_1 flows in the coaxial line through the plasma 12. After a sharp decrease in plasma conductivity, a pulsed increase in voltage is observed, which leads to an explosive emission of electrons from the end of the cathode, as a result the I_2 electron beam current arises. The accelerator operation diagram with main components and physical processes is shown in Fig. 1 (left). The coaxial electrode system consists of a tubular cathode 3 and a chamber wall 4, which is the anode. Electrodes are separated from each other by a high-voltage insulator. The power supply system of the accelerator consists of PCG 1, which is a capacitive storage device and supplies energy to the inductive storage device 10 in a pulsed mode. PCG 2 feeds PGs 6, that injects plasma into the accelerator evacuated volume, forms a conductivity region with a density of about $n_e = 10^{13}…10^{14}$ cm^{-3}. On expiry of the set time, the PCG 1 is triggered and the energy from it is fed through the air discharger *F1* to the accelerator electrode system. The current I_{PCG} of the PCG begins to flow through the plasma 12. A current-conducting channel is formed in plasma. It moves in plasma towards the end of the cathode and according to calculations it has an S-shape [15 - 17]. The IES includes the coaxial accelerator chamber up to the boundary 7, the PCG, the air discharger and connecting high-voltage cables (main circuit below). A change rate of the current in time defines the voltage multiplication factor, it can reach several kA/ns in our case.

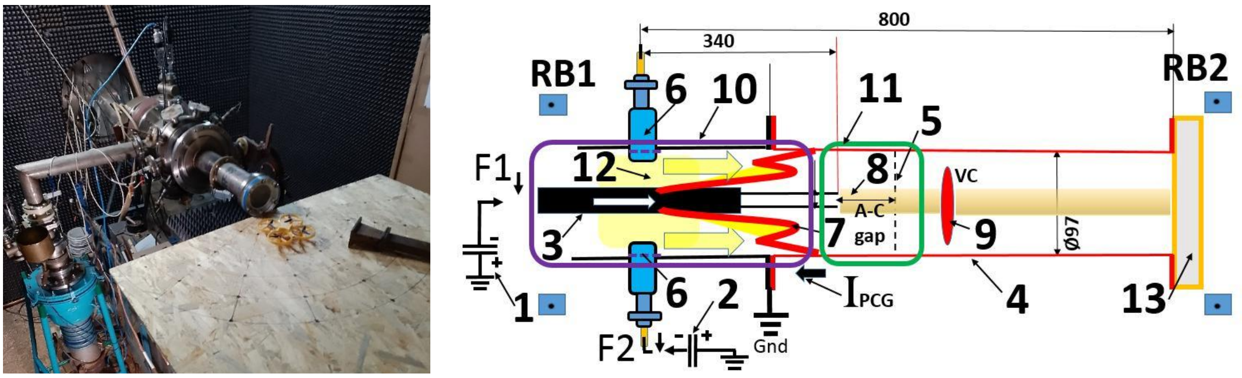

Fig. 1. DIN-2K electron accelerator general view and DIN-2K electron accelerator schematic diagram. 1 – is the PCG of main circuit; 2 – is the PCG of plasma guns block; 3 – is the tubular cathode; 4 – is the grounded accelerator chamber body, anode; 5 – is the anode mesh; 6 – is plasma guns; 7 – is the S-shaped plasma current front in the POS [15 - 17]; 8 – is the electron beam; 9 – is the virtual cathode (VC); 10 – is the inductive energy storage block; 11 – is the vacuum diode; 12 – is the POS created by PG; 13 – is the plexiglass end flange, RB1, RB2 are Rogovsky belts, Ipcg – direction of movement of the main circuit current; F1, F2 – controlled air discharges

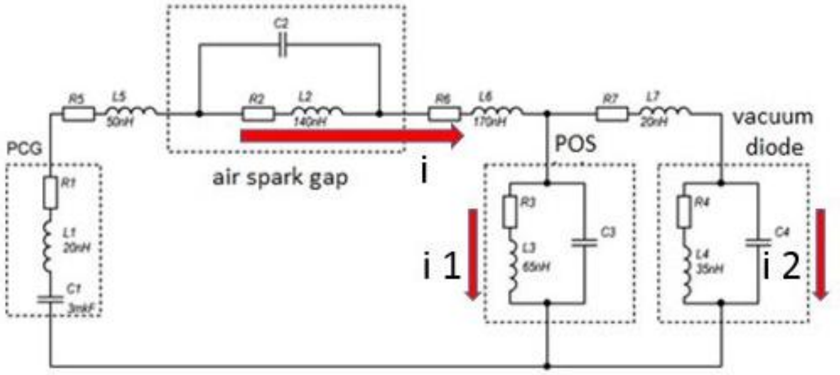

Fig. 2. Electrical equivalent circuit of the accelerator. C1 and L1 are inductance and capacitance, R1is the ohmic resistance of PCG, C2, L2, R2 are the appropriate parameters of the controlled discharger; C3, L3, R3 – for POS; C4, L4, R4 – for the vacuum diode; L5, R5 – for feeding coaxial cables; L6, R6 – for vacuum chamber before the POS; L7, R7 – for the vacuum chamber after the POS

During the POS operation, plasma resistance is increased from 0.01…0.05 Ω by approximately two orders of magnitude, which results in an abrupt drop in current, but without a final disturbance of conductivity. The greater the current time derivative, the greater the induced voltage. A decrease in the IES inductance results in an increase in the main circuit current, and an increase in the rate of its change during the POS operation. The induced voltage is applied to the end of the tubular cathode and when its value exceeds 150 kV, the conditions appear for the formation of explosive emission and the electron beam 8. The beam propagating in the waveguide and bypassing the metal grid 5, when exceeding the space-charge-limiting current (*Iscl*) forms a virtual cathode 9, which is a source of an electromagnetic radiation. The frequencies provided by the vircator can be adjusted by the size of the anode-cathode gap (A-C gap). Thus, voltage multiplication is a determining factor for ensuring the sequence of many physical processes of technological importance.

2. TECHNIQUE AND EXPERIMENTAL METHODS

2.1. DEFINING THE CURRENT AND VOLTAGE

Rogowski coils RB1 and RB2 were used for measurements of the currents in the micro- and nanosecond time ranges. In particular, for measuring the current in the energy storage phase in the IES and during POS opening, and for measuring the electron beam current. The charging voltage of PGs varied in the range of 6 to 20 kV. The charging voltage at the PCG varied in the range of 20 to 45 kV. The shape of the current curve recorded by the Rogowski coil and the recalculated voltage are shown in Fig. 3. The calculation was made based on the change in current overtime during the POS tripping. The well-known formula $U = -L\frac{dI}{dt}$ is used. $\frac{dI}{dt}$ is taken from oscillogram. L is calculated using the Thomson formula $= \frac{T^2}{4\pi^2 C}$. The calculated voltage oscillogram obtained from the experimental current oscillogram allows us to clearly define the moment of the origination and completion of the break and in this case, it is equal to 48 ns, and specify the peak time of the induced voltage, its shape and estimate the average values of the induced voltage The beginning of the current decline and its termination allowed us to estimate the average values of the induced voltage, see Fig. 3, the section with a slope angle α1. Whereas the flat sections with a sharper slope angle α2 allow us to estimate the possible maximum voltage values, which last for a much shorter period of time. The sharper the angle α1, the smaller Δt and, accordingly, the greater the rate of current change, which causes higher values of induced voltage. Based on the resolution of the oscilloscope of 5 ns, there is a possibility that the true maximum voltage values may be higher, over shorter time intervals. Due to this, in our case, it is more reliable to operate with average voltage values. The moment of the POS triggering can be determined by the beginning of the voltage curve growth. The conductivity restoration is associated with the voltage curve reaching its initial level. The lifetime of the beam can be estimated from the duration of the voltage front, here it's equal to 20 ns. This time also corresponds to the process of explosive emission. The obtained calculated data of the average values of induced voltage differ from those recorded using a capacitive voltage divider within 25%.

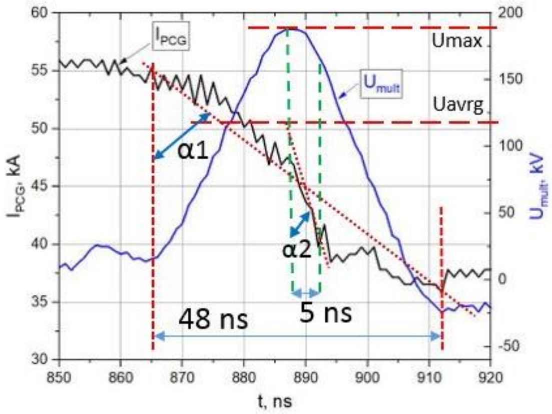

Fig. 3. The main circuit current dynamics in the POS operation time (current interruption time) and the calculated shape of the induced voltage curve

It also should be noted that considering the limited resolution of the oscilloscopes used for this purpose, which is not less than 5 ns, the peak values of the induced voltage can get higher in shorter time intervals. Therefore, when obtaining the oscillogram, its average values were also used for the estimation of the induced voltage according to the results of signal integration.

2.2. POS TRIGGERING STABILITY

To ensure the repeatability of the experiments and confirm the reliability of the data obtained on pulse-to-pulse basis, a series of experiments was conducted using different initial parameters of the main discharge circuit, and the discharge circuit of the plasma guns, and different time parameters of the delay between the operation of the PG and PCG. The data was analyzed based on the obtained current oscillograms. The comparison was carried out according to the amplitude of the currents, and their ascending and descending fronts. Fig. 4 shows the oscillograms of five pulses of the main discharge circuit in the POS operation mode. We can see that the difference in the amplitude of the maximum current of the main circuit does not exceed 5%, the spread in the current change amplitude during the triggering of the plasma opening switch does not exceed 10%. In energy accumulation mode, the dynamics of the current at the front have an absolute coincidence, which is indicative of that the current in the plasma of the POS, before its operation, moves along a stable "trajectory" and the current cord of the circuit breaker begins to "break" in the same place. The amplitude values of the main circuit current reach 75 kA, the values of the opening current are approximately 30 kA, which is 40% of the maximum value and it is indicative of sufficiently efficient operation of the POS. When testing the synchronous operation of the six involved plasma guns, it was found out that the lagging time between the first triggered gun and the last gun that is triggered with a delay in time does not exceed 700 ns (Fig. 5). Such deviations in time are not critical, considering that the time of the plasma propagation from the guns to the cathode is approximately 1 μs, and the time of the plasma generation by the guns is about 40 μs (Fig. 6). During this time, the plasma manages to fill the coaxial gap in the radial section and form a region of quasi-uniform density. Starting from the fourth half-period of the current, after 13 μs, the discrepancies in amplitude and lag are decreased. The spread in amplitude does not exceed 2.1 kA. The average total current from all the guns is varied in the range of 10 to 12 kA.

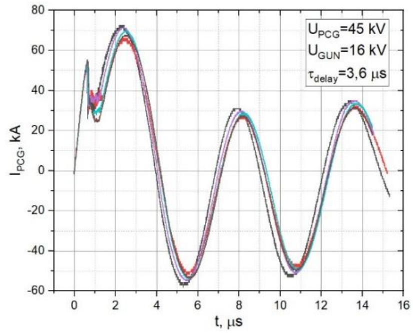

Fig. 4. Oscillograms of the five pulses of the main circuit in the POS operation mode

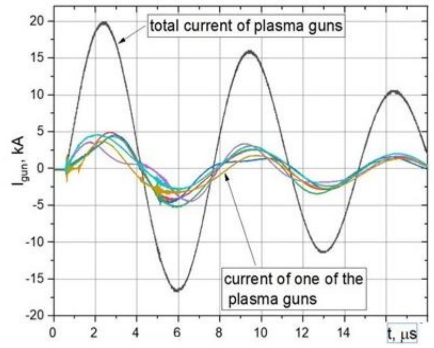

Fig. 5. Oscillograms of the current circuit of PGs and the currents of each individual gun

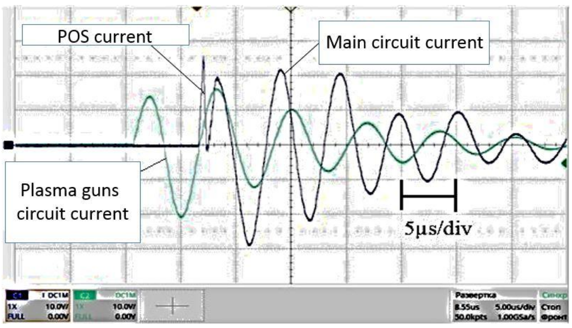

Fig. 6. Oscillograms of the main circuit in the POS operation mode and with the circuit current of PGs

Having stable current characteristics, calculating the operating speed of the plasma opening switch ΔI/Δt and knowing the inductance of the discharge circuit L, we can calculate the amplitude and specify the nature of a change in time of the induced voltage.

2.3. PROCESSES OCCURRING ON VACUUM DIODE ELECTRODES

For a clearer understanding of the processes occurring in the accelerator during the POS operation, the imprints of plasma, current and explosive emission on the cathode were analyzed including the consequences of the interaction of the beam with the grid and the end flange of the waveguide.

Fig. 7 presents a photo of the cathode. We can see that the dendrites sprout from the cathode end, which is indicative of the presence of a high overvoltage at the very edge. In the inner part of the tube, we can also observe the rolling layers of cathode material, ~ 10 mm deep, which may be due to the recoil force after a fleeting 30…100 ns explosion. The edge of the cathode has traces of melting. The formed annular beam of electrons is directed towards the grid. Upon contact with the grid, the beam forms an anode plasma. Also, the main plasma flow formed by the guns moves behind the beam at a speed of 5 cm/μs, therefore at a distance between the cathode and the grid of 10 mm, the time of unhindered existence of the beam does not exceed 25 ns. The consequence of the interaction of the beam with the grid is its melting and sublimation. The beam imprints are also observed on the plexiglass flange and have the form of a ring.

After several hundred pulses, the accelerator chamber was depressurized, and the surfaces of the electrodes of the vacuum diode were subjected to the analysis. On the surface of the cathode, we observe a zone of deposited films, i.e. the so-called deposition or emission zone formed by the material of plasma guns in the area where the plasma guns are located, see Fig. 8. This zone is uniformly sprayed and has a brownish-dark shade. The length of this area is about 205 mm, and it spreads symmetrically relative to the axis of the guns. The plasma from the guns reaches the cathode in approximately 1 μs. Before the PCG is actuated, on average it takes at least 3 μs after the triggering of the plasma guns, the plasma manages to spread up to 110 mm. The discrepancies within 25 mm are not significant. The PCG current flows through the plasma, forming a current cord that moves along the cathode. The section of movement where the current cord breaks is equal to approximately 160 mm. On this section, the plasma touching the cathode surface provides the cleaning of its surface with simultaneous spraying. The section has a uniformly brightened appearance almost to the very end of the cathode, which is approximately 145 mm, simultaneously with the beginning of the opening at the cathode end, a rapid increase in voltage occurs at a rate of ~ 5 kV/ns, while the current drop rate is ~ 400 A/ns. As a result, the voltage at the cathode end reaches values varying in the range of about 200 to 380 kV. These values are sufficient to provoke explosive emission of electrons from the cathode end. Fig. 9 shows image of the surface of the grid rods after 50 pulses. According to the results of the analysis, the primary specimen has a contaminated surface. After the treatment with alcohol, the surface of the primary specimen is still contaminated, mainly up to 91%. Carbon and oxygen are observed, which is indicative of the presence of oil films and oxides. Si, Ca, S are also present, which is indicative of the presence of a human factor, i.e. contact of the man with the surface. The main elements of the material, in particular Fe, Ni, Cr are integrally observed at the level of 6%. After 50 pulses, the distribution of the elemental composition changes significantly and we get the clean surface. The number of impurities containing C and O decreased to 29%. The percentage of Fe, Ni, Cr is increased approximately 10 times to 68%. Copper particles with sizes of 100 nm to 10 μm appear, which is a consequence of cathode erosion and explosive emission processes. The surface of the grid has traces of melting. The grid withstands about 250 pulses before its gradual destruction begins.

To form a virtual cathode, the current of the formed electron beam should exceed the vacuum critical current. The vacuum critical current or so called space-charge-limiting current is derived from the formula:

$$I_{scl} = \frac{mc^3}{e}\frac{(\gamma^{\frac{2}{3}}-1)^{3/2}}{\frac{d}{R_b}+2\ln\left(\frac{Rc}{R_b}\right)},$$

where $\gamma = 1 + \frac{eV_0}{mc^2}$, V_0 is the induced voltage on the vacuum diode or beam energy, e, m are the charge and mass of the electron, γ is the relativistic factor, Rc and R_b are the inner radius of the anode and the radius of the beam accordingly, which corresponds to the outer radius of the cathode, or slightly more due to the non-magnetization of the beam, d is the thickness of the annular beam.

Fig. 7. Photo of the processes at the cathode end (left) and photo of the interaction of the beam with the anode grid

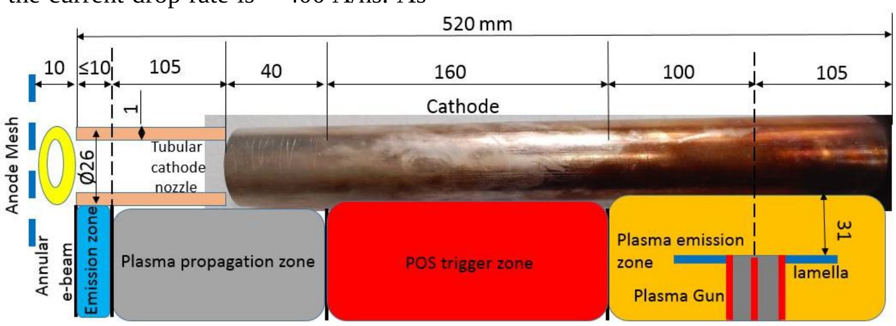

Fig. 8. General view of the explosive emission cathode with traces of current-plasma processes after 100 pulses

Fig. 10 shows the estimated calculated dependences of the values of the critical vacuum current *Iscl* as a function of the induced voltage at fixed geometric values corresponding to the real plant. Fig. 10 shows that the vacuum critical current for the expected voltages on the vacuum diode ranging from 150 to 400 kV does not exceed 2 kA, which sets a certain limit for the beam current. The beam current that obtained experimentally must be at least 2 kA. The obtained experimental dependences provide current indicators in the range of 6…12 kA. As it seen from Fig. 11 the experimentally obtained beam current at least 4 times greater of vacuum critical current that have been calculated.

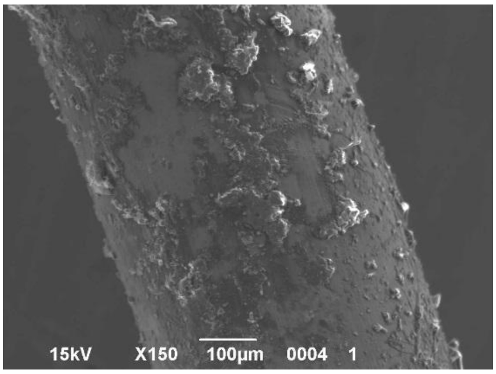

Fig. 9. Photo of the grid using the electron microscopy

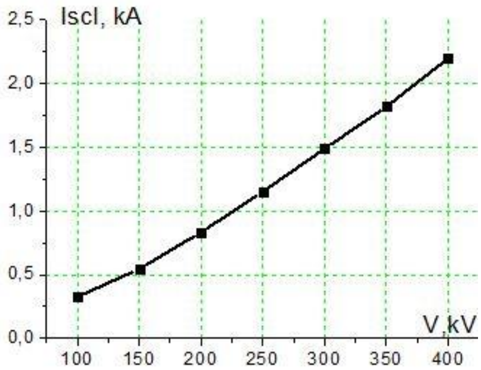

Fig. 10. Dependences of the critical current on the induced voltage

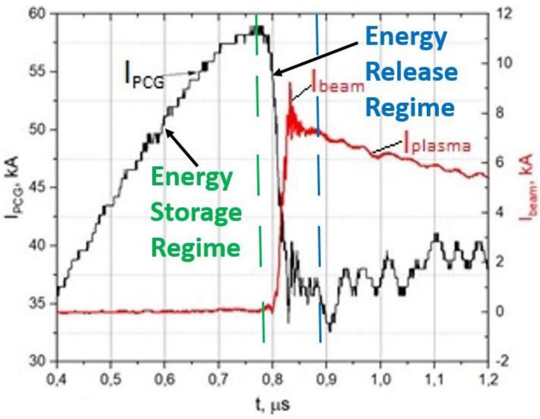

Fig. 11. Chronogram of the opening current of the POS and the beam current

To obtain a maximum induced voltage, the parameters of the circuits are as follows: $U_{PCG} = 35$ kV, $U_{PG} = 16$ kV, delay time $t_{delay} = 3.6$ µs, $p = 5\cdot10^{-5}$ Pa. The resulting multiplication factor was $k = 8.5$. The induced voltage was 297 kV.

3. EXPERIMENTAL PART

3.1. DEPENDENCE OF THE CURRENT CHARACTERISTICS AND INDUCED VOLTAGE ON THE PARAMETERS OF THE MAIN CIRCUIT

To reveal the effect of the main circuit voltage (PCG charging voltage) on the POS opening rate, POS breaking current, POS opening time, the voltage induced during the opening time, and the voltage multiplication factor, all operating parameters were fixed values. The plasma gun capacitors were charged to 16 kV. The PCG was triggered with a delay of 3.6 µs. The vacuum conditions were not worse than $3\cdot10^{-3}$ Pa. The main circuit charging voltage was changed from 15 to 45 kV in steps of 5 kV. The pulses with fixed parameters were repeated at least 5 times. Figs. 12, 13 shows the dependences of the current dynamics of the main discharge circuit for different PCG discharge voltages.

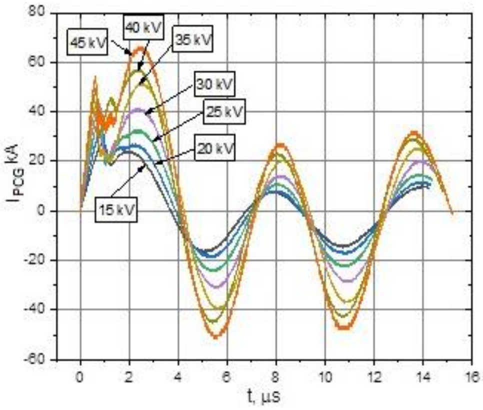

Fig. 12. Time dependence of the main circuit current for different PCG voltages

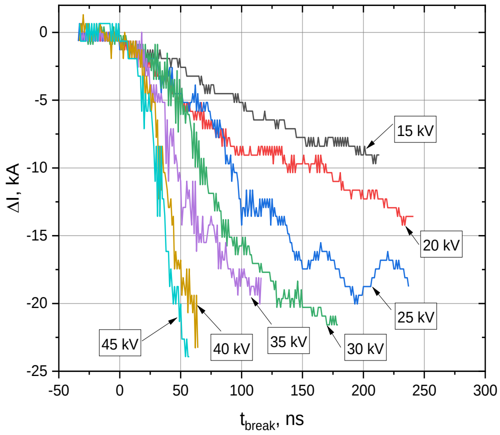

Fig. 13. Rate of change in the POS current for different PCG voltages

The main output parameters were studied during the POS opening at a vacuum of $(6\cdot10^{-5}…3\cdot10^{-3})$ Pa and a diode gap of 8 mm. The POS opening current is equal to ΔI, and it is calculated by the difference between the upper and lower values of the current at the POS opening stage (see Figs. 14 and 4). To do this calculation, a straight section of the current was chosen in the POS opening stage, where di/dt is maximum. ΔI [kA] is the value of the opening current, where di/dt is maximum. t_{break} is the opening time, where di/dt is maximum. $U_{average}$ is the calculated average induced voltage. Ldi/dt and $k_{mult} = U_{average}/ U_{PCG}$ is the multiplication factor.

As can be seen from Fig. 14, increasing the charging voltage allows us to reliably obtain voltage multiplication factors k_{mult} = 6, and an induced voltage sufficient for the explosive emission from the cathode to take place. Fig. 15 shows the dependence of the opening time of the POS on the voltage. The POS opening time has decreased significantly with an increase in voltage, according to the exponential tendency. Thus, at a voltage of 45 kV, the opening time is decreased almost threefold to 50 ns compared to that for the voltage of 15 kV. Fig. 16 shows that an increase in inductance due to the reduction of the number of connecting power cables (marked in Fig. 16 by 1, 2, ..., 6) results in an increased angle of inclination of the current on its decline during the operation of the circuit breaker and thus to a decrease in the induced voltage and the multiplication factor.

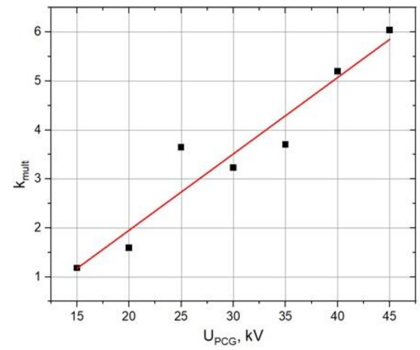

Fig. 14. Dependence of the multiplication factor on the main circuit voltage

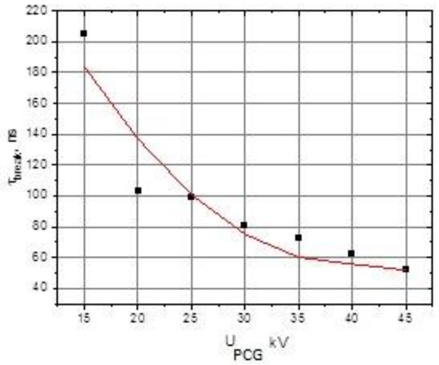

Fig. 15. Dependence of the POS opening time on the main circuit voltage

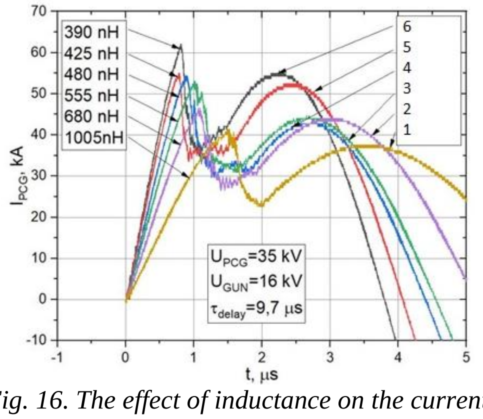

Fig. 16. The effect of inductance on the current value of the main circuit and the angle of the curve during POS operation

The energy accumulation time decreases with increasing charging voltage.

3.2. THE EFFECT OF THE PARAMETERS OF THE DISCHARGE CIRCUIT OF PLASMA GUNS ON THE MAGNITUDE OF THE CURRENT OF THE MAIN DISCHARGE CIRCUIT

An important element of the accelerator is the block of PGs, which injects plasma into the coaxial system of the accelerator, forming a plasma bridge of the POS. In the experiment, the capacitor of the main circuit of the PCG was charged to 35 kV, the charging voltage on the capacitors of the guns was changed from 6 to 20 kV in steps of 2 kV. The vacuum in the accelerator chamber was not worse than $3 \cdot 10^{-3}$ Pa. Fig. 17 shows the dependences of the main circuit current with the activation of the PCG for different values of the voltage on the PGs.

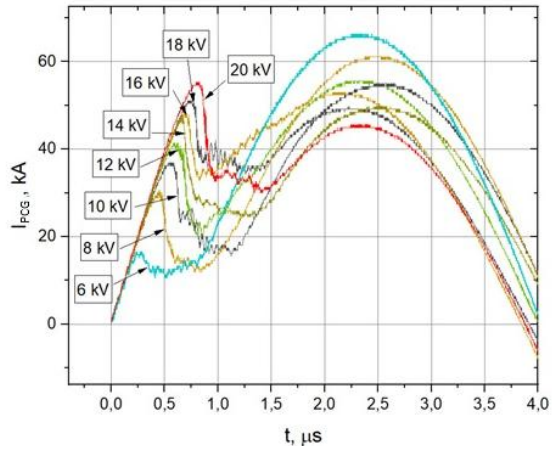

Fig. 17. Dependence of the main circuit current on time as a function of the discharge voltage of PGs

We can see that an increase in the voltage on the guns results in a change of the amplitude of the main circuit current, increasing it almost three times when comparing the current curves for 6 and 20 kV. The amplitude of the opening current of the POS differs by five times at the same values of the discharge voltage. The dependences of the main circuit current during the operation of the POS on different values of the voltage on the PGs at a POS voltage of 35 kV and other equal conditions are shown on Figs. 18, 19. The use of low voltages on PGs is unacceptable and ineffective from the point of view of ensuring the voltage multiplication. It should be noted that starting from 8 kV and above the reduction in the opening time is not observed.

Fig. 18 also shows that the angle of inclination of the current curves during the tripping of the circuit breaker is almost the same for all the values of the charging voltage except for 6 kV, which is indicative of the same values of the average induced voltage and the absence of a significant effect on the speed of the current tripping for the charging voltage of PGs.

Fig. 20 gives the time dependences of the number of guns used for the POS feeding at positive and negative polarity of the central rod electrode. The number of guns, their increase from one to six allows us to increase the amplitude of the main circuit current by 1.8 times. However, their number does not have a significant effect on the current change rate, except for the use of less than three guns.

The number of guns is more important, increasing their number from one to six allows us to increase the amplitude of the main circuit current by a factor of 1.8. Changing the number of guns, or their type, which could provide a higher plasma density and its more uniform distribution in the volume requires further research and improvements.

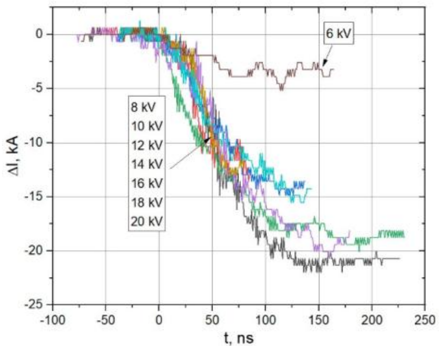

Fig. 18. Rate of change of the POS current (during current interruption) for different PG voltages

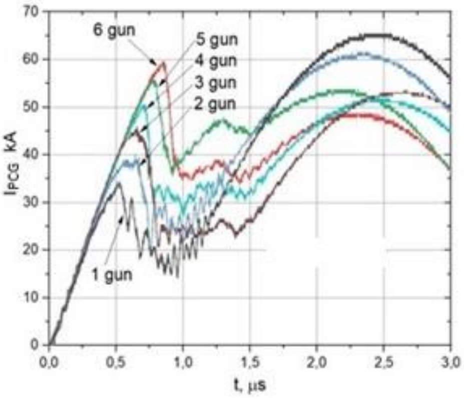

Fig. 19. Time dependence of the main circuit current for different numbers of PGs used to power the POS

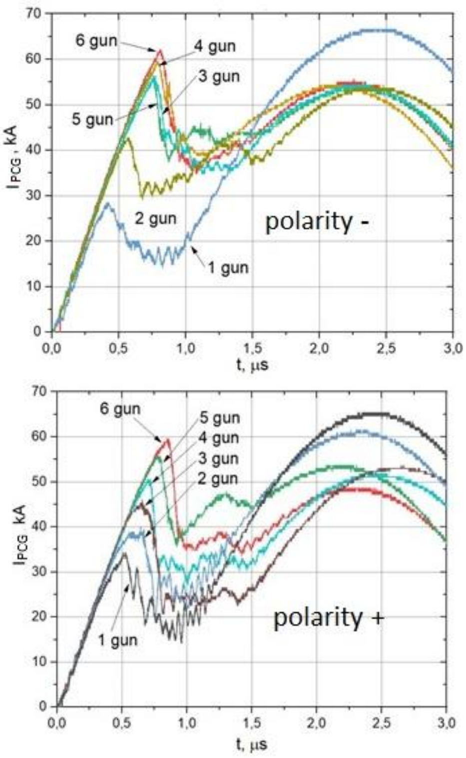

Fig. 20. Time dependence of the number of PGs used to power the POS at positive and negative polarity of the central rod electrode

Fig. 20 also shows that the amplitude values of the main circuit current are larger, by approximately 5%, when using negative polarity. Although differences in polarity can be found, they cannot be considered as significant for this geometry of the guns.

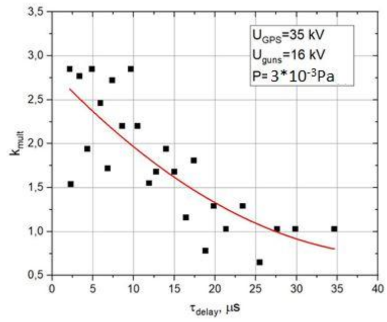

Fig. 21. The dependence of delay time on the value of the multiplication factor

An experimental approximation curve of the effect of the delay time on the value of the multiplication factor has been obtained, see Fig. 21. When changing the delay time between the operation of the PGs and the main circuit of the POS in the range of 2 to 30 μs with a step of 1 μs, it was established that the highest multiplication factors are in the time interval not exceeding 10 μs.

CONCLUSIONS

The method of determining the induced voltage from the current oscillograms during the operation of the plasma opening switch was improved using an increased resolution of the Rogowski belt integrator. Thus, it was possible to eliminate the need for the arrangement of the capacitive voltage divider plates in the internal volume of the chamber, which can affect the studied physical processes.

A maximum multiplication factor is 8.5 at a voltage of the main circuit of 35 kV. In this case, the maximum currents of the main circuit varied in the range of 70 to 100 kA, the POS opening currents are equal to 30 kA, and the induced voltage is 297 kV. Current beams with values of 6…12 kA and exceeding those of the limiting vacuum current have been obtained for the selected diode geometry.

It has been established that it is possible to obtain the values of the induced voltage that will result in the explosive emission and formation of an electron beam current exceeding the critical vacuum current by increasing the voltage of the main circuit and selecting the optimal voltage values of the circuit that feeds the plasma guns.

From the point of obtaining the maximum induced voltage, the optimal parameters for DIN-2K IES with POS are as follows: U_{PCG} exceeding 35 kV, U_{PG} = 20 kV, delay time less than 10 μs, and the vacuum not worse than $3\cdot10^{-3}$ Pa. An increase in the value of the discharge voltage from 15 to 45 kV results in an increase of the interruption rate and the curve has more equal sections, which is indicative of higher coefficients of voltage multiplication and the maximum values of the current of the main circuit are increased. An increase in the voltage results in a linear increase in the multiplication factor. Reducing the inductance and increasing the number of plasma guns results in an increase in the output parameters of the accelerator.

ACKNOWLEDGEMENTS

The authors are grateful to P.V. Mateychenko (Institute for single crystals) for the SEM studies.

REFERENCES

1. J. Benford, J.A. Swegle, E. Schamiloglu. *High power microwaves.* CRC Press, 2015, 447 p.
2. S. Mumtaz, H.S. Uhm, E.H. Choi. Progress in vircators towards high efficiency: Present state and future prospects // *Physics Reports.* 2024, v. 1069, p. 1-46.
3. D.V. Vinnikov, V.V. Katrechko, V.B. Yuferov, V.I. Tkachev. Plasma guns of an erosion type with the pulse-periodic gas-metal injection // *Problems of Atomic Science and Technology.* 2022, № 6, p. 60-65.
4. D.V. Vinnikov, V.V. Katrechko, O.M. Ozerov, V.I. Tkachev, S.V. Marchenko V.B. Yuferov, O.V. Manuilenko. Influence of the energy parameters of the primary circuit on the current characteristics of the DIN-2K accelerator // *Problems of Atomic Science and Technology.* 2023, № 4, p. 36-40.
5. D.V. Vinnikov, V.V. Katrechko, O.V. Manuilenko, O.M. Ozerov, I.N. Onishchenko, V.I. Tkachev, V.B. Yuferov, S.V. Marchenko. Improving the functionality of the small-dimension accelerator DIN-2K with a plasma opening switch // *Problems of Atomic Science and Technology.* 2024, № 3, p. 60-66.
6. V.V. Katrechko, D.V. Vinnikov, O.V. Manuilenko, O.M. Ozerov, I.N. Onishchenko, V.I. Tkachev, V.B. Yuferov, S.V. Marchenko. Radiation in the microwave range at pulse accelerators with virtual cathode generator // *Problems of Atomic Science and Technology.* 2024, № 3, p. 79-83.
7. A.G. Lynn, M. Gilmore, N.R. Devarapalli, M.E. Savage, B.S. Stoltzfus. Interferometric measurements on a triggered plasma opening switch source *// IEEE Pulsed Power Conference Publication Year*. 2009, p. 652-657.
8. O.S. Druj, V.V. Yegorenkov, A.V. Shchagin, V.B. Yuferov. Electron beam transport in dielectric tubes // *East European Journal of Phisics.* 2014, v. 1, № 1, p. 70-73.
9. O.V. Manuilenko, A.V. Pashchenko, V.G. Svichensky, B.V. Zajtsev. High-current relativistic electron beam focusing in plasma // *Problems of Atomic Science and Technology.* 2021, № 4, p. 30-34.
10. O. Manuilenko, V. Novikov, A. Pashchenko, I. Pashchenko, I. Shapoval, V. Yuferov. Effect of electron collisions with residual neutral gas on characteristic oscillation frequencies in systems of electron flows with a virtual cathode // *Problems of Atomic Science and Technology*. 2023, № 4, p. 33-35.
11. S.N. Dubniuk, R.A. Anokhin, A.F. Dyachenko, A.P. Кobets, A.I. Kravchenko, O.V. Manuilenko, К.V. Pavlii, V.N. Reshetnikov, A.S. Shevchenko, V.A. Soshenko, S.S. Tishkin, B.V. Zajtsev, A.V. Zhuravlyov, V.G. Zhuravlyov. Radiation complex on the basis of helium ions linac // *Problems of Atomic Science and Technology.* 2018, № 4, p. 46-51.
12. A.F. Dyachenko, R.A. Anokhin, S.N. Dubniuk, A.P. Кobets, A.I. Kravchenko, O.V. Manuilenko, V.M. Reshetnikov, V.A. Soshenko, S.S. Tishkin, B.V. Zajtsev, O.V. Zhuravlov, V.G. Zhuravlov. The bunch formation and transport system to the target of the helium ions LINAC // *Problems of Atomic Science and Technology*. 2018, № 4, p. 52-55.
13. O.V. Bogdan, V.I. Karas’, E.A. Kornilov, O.V. Manuilenko. 2.5-dimensional numerical simulation of a high-current ion linear induction accelerator // *Plasma Physics Reports*. 2008, v. 34, № 8, p. 667-677.
14. O.V. Bogdan, V.I. Karas’, E.A. Kornilov, O.V. Manuilenko. High-current ion induction LINAC for heavy ion fusion: 2D3V numerical simulation // *Problems of Atomic Science and Technology*. 2008, № 6, p. 110-114.
15. O.V. Manuilenko, I.N. Onishchenko, A.V. Pashchenko, I.A. Pashchenko, V.B. Yuferov. Current flow dynamics in plasma opening switch // *Problems of Atomic Science and Technology.* 2021, № 4, p. 6-10.
16. O.V. Manuilenko, I.N. Onishchenko, A.V. Pashchenko, I.A. Pashchenko, V.A. Soshenko, V.G. Svichensky, V.B. Yuferov, B.V. Zajtsev. Magnetic field dynamics in plasma opening switch // *Problems of Atomic Science and Technology*. 2021, № 6, p. 61-66.
17. O.V. Manuilenko, I.N. Onishchenko, A.V. Pashchenko, I.A. Pashchenko, V.B. Yuferov. Plasma and magnetic field dynamics in POS: PIC simulations // *Problems of Atomic Science and Technology*. 2022, № 6, p. 55-59.

Article received 28.05.2025

ЕКСПЕРИМЕНТАЛЬНЕ ДОСЛІДЖЕННЯ ПЛАЗМОВОГО КОМУТАТОРА СТРУМУ НА ПРИСКОРЮВАЧІ З ІНДУКТИВНИМ НАКОПИЧУВАЧЕМ ЕНЕРГІЇ

Д.В. Вінніков, О.М. Озеров, В.В. Катречко, В.І. Ткачов, С.В. Марченко, В.Б. Юферов, О.В. Мануйленко, І.М. Оніщенко

Проведене експериментальне дослідження плазмового комутатора струму (ПКС), його динаміки на малогабаритному електронному прискорювачі прямої дії з індуктивним накопичувачем енергії (ІНЕ). Використано методику визначення індукованої напруги за експериментальними осцилограмами струму. Одержано характерні осцилограми струмів. Встановлені значення зарядної напруги та струму основного розрядного контуру, що забезпечують максимальну індуковану напругу та найбільші коефіцієнти її множення. Визначений вплив зарядної напруги контуру плазмових гармат та кількості гармат на множення напруги. Визначені оптимальні часи затримки між спрацьовуванням плазмових гармат та генератором імпульсних струмів основного контуру. Визначено вплив індуктивності на коефіцієнт множення напруги. Одержані струми пучків електронів зі значеннями, що перевищують граничний вакуумний струм, для обраної геометрії вакуумного діода.